Hypermethylation of RAD9A intron 2 in childhood cancer patients, leukemia and tumor cell lines suggest a role for oncogenic transformation

Danuta Galetzka (✉ Danuta.Galetzka@unimedizin-mainz.de)
Johannes Gutenberg Universitat Mainz https://orcid.org/0000-0003-1825-9136
Julia Boeck
Institute of Human Genetics, Julius Maximilians University Würzburg
Marcus Dittrich
Bioinformatics Department Julius-Maximilians-Universitat Wurzburg
Olesja Sinizyn
Department of Radiation Oncology and Radiations Therapy , University Medical Centre, Mainz
Marco Ludwig
DRK Medical Centre Alzey
Heidi Rossmann
Institute of Clinical Chemistry and Laboratory Medicine, University Medical Centre, Mainz
Claudia Spix
German Childhood Cancer Registry, Institute of Medical Biostatistics, Epidemiology and Informatics, University Medical Centre, Mainz
Markus Radsak
Departement of Hematology, University Medical Centre, Mainz
Peter Scholz-Kreisel
Institute of Medical Biostatistics, Epidemiology and Informatics, University Medical Centre, Mainz
Johanna Mirsch
Radiation Biology and DNA Repair, Technical University, Darmstadt
Matthias Linke
Institute of Human Genetics, University Medical Centre, Mainz
Walburgis Brenner
Departement of Obsterics and Womans Health, University Medical Centre, Mainz
Manuela Marron
Leibniz Institute for Prevention Research and Epidemiology, BIPS, Bremen
Alicia Poplawski
Institute of Medical Biostatistics, Epidemiology and Informatics, University Medical Centre, Mainz
Dirk Prawitt
Center for Pediatrics and Adolescent Medicine, University Medical Centre, Mainz
Thomas Haaf
Institute of Human Genetics, Julius Maximilians University, Würzburg
Heinz Schmidberger
Department of Radiation Oncology and Radiation Therapy, University Centre, Mainz

Research article

Keywords: RAD9A, childhood cancer, hypermethylation, normal body cells, somatic mosaicism, leukemia

Posted Date: August 12th, 2020

DOI: https://doi.org/10.21203/rs.3.rs-55470/v1

Abstract

Background: Most childhood cancers occur sporadically and cannot be explained by an inherited mutation or an unhealthy lifestyle. This suggests other predisposition defects that may support the oncogenic transformation of cells, e.g. via impaired DNA-repair. Our study consequently aims to investigate the impact of increased methylation of intron 2 of RAD9A in cancer patients which may be associated with oncogenic transformation.

Methods: We performed an epimutation screen of RAD9A and other candidate genes (APC , CDKN2A , EFNA5 , and TP53) using bisulfite pyrosequencing and deep bisulfite sequencing (DBS) in skin fibroblasts of 20 patients with primary cancer in childhood and second primary cancer (2N) later in life, 20 matched patients with only one primary cancer (1N) in childhood and 20 matched cancer-free (0N) controls. Furthermore, we analyzed leukemia cancer samples, tumor cell lines, EBV lymphoblasts and FaDu subclones. Radiation, colony formation assays, cell proliferation, PCR and molecular karyotype SNP-array experiments were performed. Data were analyzed using the Kruskal-Wallis rank-sum test, Benjamini-Hochberg procedure, REML and R-scripts.

Results: Four 1N patients and one 2N patient displayed elevated mean methylation levels (>10%) in intron 2 of RAD9A . DBS of RAD9A in these patients revealed >2% hypermethylated alleles consistent with relevant epimutations. We found RAD9A hypermethylation in the bone marrow of patients with pre-ALL (pre-acute lymphoblastic leukemia), AML (acute myeloid leukemia), NHL (non-Hodgkin lymphoma), PBL (plasmablastic lymphoma) and EBV-(Epstein Barr virus) transformed lymphoblastoid cells. Molecular karyotyping of AML samples with hypermethylated RAD9A showed an evolving duplication of 1.8 kb on Chr16p13.3 including the PKD1 gene. In generated FaDu subclones with hypermethylated RAD9A, we found a homozygous inactivation of CHD2, SPATA8 , SMARCA1 and a 302 kb duplication including genes deregulated in cancer. The detected aberrations proved to influence cell viability. RAD9A methylation was not affected by radiation or the chemotherapeutical daunorubicin.

Conclusion: The analysis of patient samples, cell lines and subclones suggest a connection between methylation levels of the RAD9A intron 2 locus and inactivation or amplification of important genes and survival of the cells. We propose that RAD9A epimutations may have an impact on leukemia, tumorigenesis, cancer progression and can potentially serve as a valuable biomarker.

Background

Tumorigenesis is a multistep process, involving an accumulation of genetic and epigenetic changes in multiple genes resulting in both, the inactivation of tumor suppressor (TS) genes and/or activation of oncogenes [1]. Tumor epigenomes are characterized by a global loss of DNA methylation, leading to reactivation of retrotransposons and genome instability, as well as regional hypermethylation and silencing of TS genes, compromising DNA repair and cell cycle control [2]. In sporadic cancer (epi)genetic changes, which may arise by stochastic DNA replication errors or adverse environmental exposures, are usually restricted to the tumor and its precursor cells. In contrast, most hereditary forms of cancer are caused by germline mutations in tumor suppressor genes, predisposing patients to tumor development, which itself is triggered by inactivation of the second TS allele. Accumulating evidence suggests that similar to germline mutations, constitutive epimutations involving soma-wide hypermethylation of tumor suppressor genes in normal body cells, can cause phenocopies of cancer syndromes such as hereditary non-polyposis colon cancer (HNPCC) as well as breast- and ovarian cancer [3, 4]. Since constitutive epimutations usually occur in a mosaic state with variable proportions of affected cells in different tissues, they are most likely not transmitted through the germline but may arise during early development. For some cancer-predisposing genes, i.e. *MLH1*, *MSH2*, and *DAPK1*, the probability for de novo epimutations depends on cis-regulatory genetic sequence variants [5–7].

Compared to the aging population, cancer is rare among children and young adults, representing < 1% of all cancers. Children are usually not exposed to an unhealthy lifestyle or an adverse environment, and only 5–10% of children with cancers carry predisposing germline mutations [8]. Therefore, most childhood cancers should occur sporadically. One possible explanation for the onset of sporadic childhood cancers is somatic mosaicism. A high proportion of human preimplantation embryos are chromosomal mosaics of normal and aneuploid cells [9]. One embryonal cell carrying a de novo genetic mutation can be propagated into different tissues and organs during somatic development, persist for many years and manifest earlier or later in life, depending on the amount of stem cell divisions [10]. The prenatal origins hypothesis postulates, that childhood cancers arise from postnatally persisting embryonal or more differentiated cells that carry predisposing mutations [11] and several studies have demonstrated prenatal oncogenic events underlying acute leukemia in childhood [12, 13]. During each cell division, both the DNA sequence and its epigenetic modifications are transmitted to the daughter cells. Considering that the error rate during this copying process is at least one magnitude higher for epigenetic information than for genetic information [14], constitutive epimutations may occur much more frequently than prenatal DNA sequence mutations. Mosaic constitutional *BRCA1* methylation is detected in 4–7% of newborn females without germline *BRCA1* mutations. While the cause of such

methylation is poorly understood, mosaic normal tissue *BRCA1* methylation is associated with a 2-3-fold increased risk of high-grade serous ovarian cancer (HGSOC) [15]. We have previously described monozygotic twin sisters discordant for childhood leukemia and a constitutive mosaic epimutation in the *BRCA1* TS gene [16]. Furthermore, we could show that affected fibroblasts phenotypically resemble cancer-associated fibroblasts (CAF) [17]. Based on our previous expression findings [18] we performed an epimutation analysis of *RAD9A* in a unique cohort, consisting of fibroblasts derived from individuals who survived childhood cancer and subsequently developed a second primary cancer (2N) and matched (first tumor, manifestation age, sex) individuals with childhood cancer but without second cancer (1N). Moreover, fibroblasts of 20 age- and gender-matched, cancer-free individuals served as controls (0N). Furthermore, to estimate the pathological significance of our findings we analyzed the *RAD9A* gene methylation in leukemia cancer samples, tumor cell lines and generated FaDu subclones with divergent methylation values of *RAD9A*.

Materials And Methods

Patient samples and cell lines

With the help of the German Childhood Cancer Registry, 20 individuals who survived a childhood malignancy and then developed a second primary cancer (2N) and 20 carefully matched (first tumor, manifestation age, sex) individuals who survived a childhood cancer without developing a second malignancy (1N) were recruited for the KiKme study (Cancer in Childhood and Molecular Epidemiology). Twenty matched patients (sex and age) without cancer from the Department of Accident Surgery and Orthopedics served as controls (0N). This study was approved by the Ethics Committee of the Medical Association of Rhineland-Palatinate (no. 837.440.03 [4102]; no. 837.262.12 [8363-F]; and 837.103.04 [4261]). Written informed consent to use primary fibroblasts for research purposes was obtained after genetic counseling for all participating patients.

All patients were followed up from primary cancer diagnosis to recruitment for this study several years after treatment. The primary malignancies included eleven patients with acute lymphatic or myeloid leukemia, five patients with Hodgkin- or Burkitt Lymphoma, and four patients with solid tumors. The second cancers in the 2N group were myelodysplastic syndromes, lymphoma, thyroid cancer, and solid tumors. The mean age at diagnosis of cancer were 7.2 ± 4.3 years (first diagnosis) and 15.2 ± 5.9 years (second diagnosis) for the 2N patients and 7.5 ± 4.4 years (first diagnosis) for the 1N patients. The age at fibroblast collection was 27.1 ± 3.7 years for the 2N patients and 26.3 ± 4.4 years for the 1N. The corresponding tumor samples were not available.

Affymetrix array SNP analysis [18] of 1N and 2N patients did not reveal detectable copy number variations in relevant tumor suppressor genes (*BRCA1*, *BRCA2*, *RAD9A*, *TP53*, *NF1*) or oncogenes (*PTPN11*, *ETV6-RUNX1*, *TCF3-PBX1*). No pathological germline *TP53*, *RAD9A, BRCA1, or BRCA2* mutations were identified by Sanger sequencing using the ACMG criteria (*TP53* Mutation Database (http://p53.iarc.fr/); https://www.ncbi.nlm.nih.gov/clinvar/ and https://www.lovd.nl/). *RB1* gene analysis in patient 1N20 did not reveal a pathological mutation. Using bisulfite pyrosequencing, none of the matched (1N or 2N) childhood cancer patients of this study showed *BRCA1* hypermethylation, consistent with an epimutation [16]. Cell lines 0N24 and 2N24 were derived from a pair of discordant monozygotic twins. One twin suffered from childhood leukemia and later on from a thyroid carcinoma whereas her sister is completely healthy till now.

Epstein Barr virus (EBV) transformation of resting B cells (in peripheral blood lymphocytes) to obtain proliferating immortal lymphoblastoid cells is widely used. Lymphoblastoid cells were generated in our routine labor and harvested in an early passage after stable infection. Bone marrow samples (excess material from routine chromosome diagnostics) were obtained from 27 patients with NHL (19 males, 8 females, aged 58.0 ± 12.0 years), 27 AML (16 males and 11 females, aged 60.0 ± 11.0 years), one pre-B-ALL (46,XY,t(9;22)(q34;q11.2)[2]/46,XY[25], one AML (46,XY,der(7)(q-).ish del(16)(q22)[12]/ 46,XY[10], and one plasmablastic lymphoma (PBL) with complex aberrations in 60% of cells, consisting of a hypodiploid clone (28%) and a hyperdiploid line (32%). The analysis of the samples was approved by the Ethics Committee of the Medical Association of Rhineland-Palatinate (no. 2019–14677).

The FaDu tumor cell line (from hypopharyngeal carcinoma), carrying mutations in *CDKN2A* (c.151-1G > T), *TP53* (c.376-1 G > A; c.743G > T) and *SMAD4* (c.1_1659del1659) was purchased from ATCC and characterized using SNP-array analysis in 24.05.18. The cell line BT-549 (from ductal carcinoma) was purchased from CLS (Eppelheim, Germany). The cell line, EFO21 (from ovarian serous cystadenocarcinoma), from DSMZ (Braunschweig, Germany) and the cell lines MCF7 (from breast carcinoma) and T47D (from breast cancer) were purchased from ATCC (Manassas, VA, USA). All cell lines were verified using the STR-analysis (DMSZ German Collection of Microorganisms and Cell Cultures GmbH on 21.11.2018).

Cell culture and irradiation

Primary fibroblasts from skin biopsies were cultured in Dulbecco`s Minimal Essential Medium with Earle's salts DMEM (Invitrogen, Karlsruhe, Germany), supplemented with 15% fetal bovine serum (FBS) (Merck, Darmstadt, Germany), 1% vitamins and 1% antibiotics (penicillin/streptomycin) (Biochrom, Berlin, Germany) in a 90% humidified incubator with 5% CO_2 at 37 °C.

The FaDu tumor cell line was cultured in Dulbecco`s Minimal Essential Medium (Sigma-Aldrich, St. Louis, USA) containing 1% non-essential amino acids (Biochrom, Berlin, Germany), 15% FBS (Biochrom, Berlin, Germany) and 1% antibiotics (Biochrom, Berlin, Germany). Passaging was done using 0.05% trypsin with 0.1% ethylene-diamine-tetra-acetate (EDTA) (Biochrom, Berlin, Germany). FaDu derived single-cell clones were generated by dilution of the primary cell line and propagated in DMEM (Invitrogen, Karlsruhe, Germany), supplemented with 15% FBS, 1% vitamins and 1% antibiotics (Biochrom, Berlin, Germany) using 96-well plates (Cellstar, Greiner GmbH, Kremsmünster, Germany). After 48 h wells with only one cell were selected via microscopic examination. Subsequent propagation was performed in conditioned medium (one day old medium of primary culture at 50% confluency, sterile filtered using 0.2 µm filter). The cells were transferred when they reached 80% of confluency, initially into a 24-well plate, later in a 6-well and finally in the 10 cm petri dishes

All cell lines (MCF7, BT-549, EFO21 und T47D) were cultivated in RPMI1640 (Gibco, Life Technologies, Darmstadt, Germany) supplemented with 2.5% HEPES buffer (Sigma, Darmstadt, Germany) and 1% antibiotics (Life Technologies, Darmstadt, Germany). BT-549, MCF7 and T47D were additionally supplemented with 10% FBS, EFO21 with 20% FBS.

All experiments using the primary fibroblasts were performed with growth-arrested cells in the G0/G1 stage. Confluency was achieved by contact inhibition and subsequent cultivation for two weeks and confirmed by FACS (flow cytometric cell cycle) analysis. For comparisons of 2N, 1N, and 0N patients, fibroblasts with a similar passage number 5 (± 2) were used.

Cells were exposed to X-rays with a D3150 X-Ray Therapy System (Gulmay Ltd, Surrey, UK) at 140 kV and a dose rate of 3.62 Gy/min at room temperature. Sham irradiated control cells were kept at the same conditions in the radiation device control room. The FaDu tumor cell line was irradiated at 80% of confluency. Cells were exposed to single doses ranging from 2–8 Gy and harvested at 15 min, 2 h, and 24 h after irradiation. For fractionalized irradiation, fibroblasts were irradiated 4x, 8x, or 10x with doses of 2 Gy and 4 Gy, within 20 days. Cells were given one day of recovery time between exposures and the medium was changed twice a week. Cells were harvested one day after the final irradiation.

Bisulfite Pyrosequencing

Genomic DNA was isolated with the NucleoSpin tissue kit (Macherey-Nagel, Germany). Bisulfite conversion of 0.2 µg DNA was performed with the EpiTect Bisulfite Kit (Qiagen, Germany) according to the manufacturer's instructions. PCR and sequencing primers for the genes mentioned above were designed with PyroMark Assay Design 2.0 software (Qiagen, Germany) (supplementary Table 1). The 50 µl PCR reactions consisted of 25 µl Pyro PCR Mix 2x, 5 µl Coral load 10x, 1 µl of each forward and reverse primer (10 µM), 17 µl PCR-grade water and 1 µl (~ 100 ng) bisulfite-converted template DNA (PyroMark PCR Master Mix, Qiagen). PCR amplifications were performed with an initial denaturation step at 95 °C for 5 min, 35 cycles of 95 °C for 30 sec, (60 °C for 45 sec for *RAD9A*) and 72 °C for 45 sec and a final extension step at 72 °C for 10 min. Bisulfite pyrosequencing was performed on a PyroMark Q96 MD Pyrosequencing System using the PyroMark Gold Q96 CDT Reagent Kit (Qiagen, Germany) and 0.5 µl of sequencing primers (10 µM). Data analysis was performed with the Pyro Q-CpG software (Qiagen, Germany). Single CpG errors which arise presumably due to bisulfite conversion errors (technical variation) were in the order of 1%. This value was calculated by analyzing samples of three patients in three replicates.

Data were analyzed using the Kruskal-Wallis rank sum-test. We considered the differences only statistically significant after the adjustment of p-value by the method of Benjamini and Hochberg.

Analysis of the AML and NHL patient data was performed using the Mann-Whitney-U Test (RV3.6.2)

Deep bisulfite sequencing (DBS)

Next-generation sequencing (NGS) libraries for DBS were generated as described previously [3]. PCR amplification of *APC*, *CDKN2A*, *TP53*, and *RAD9A* was performed using primers containing a target-specific part and partial adapter overhangs (supplementary Table 2). Following the purification of the amplicons with magnetic beads (0.9:1), the DNA concentration was determined with the dsDNA BR Assay System (Life Technologies, USA). Samples were diluted to 0.2 ng/µl in a total volume of 15 µl each. After pooling, barcoding was performed by PCR with NEBNext Multiplex Oligos for Illumina, Dual Index Primer Set 1 (New England BioLabs, Germany), followed by another bead cleaning step (0.9:1). DNA concentration and fragment length were determined with the High Sensitivity DNA kit on a 2100 Bioanalyzer (Agilent Technologies, USA). All barcoded pools were diluted to 2 nM and pooled to the final library. Denaturation and

preparation of the library and PhiX control were done according to the manufacturer's protocol (Illumina, USA). Paired-end sequencing was performed on an Illumina MiSeq using the MiSeq Reagent Kit v2 (2 × 150 cycles) cartridge.

DBS Analysis: The sequences in FASTQ format were processed using the Amplikyzer2 [19] pipeline, which provides a detailed nucleotide-level analysis including the calculation of CpG methylation rates. All sequences were aligned to the genomic sequence of each amplicon using default settings. For the subsequent extraction of reads and CpG-wise methylation status only reads with an overall bisulfite conversion rate of over 95% were considered. Further downstream processing of Amplikyzer2 output files and subsequent analyses of methylation rates were performed using R-scripts. Statistical analyses were performed with the statistical software package R (Version 3.2.2).

SNP array (molecular karyotype) analysis

High-resolution screening for microdeletions and duplications of the FaDu cell line and subclones was performed with the Affymetrix GeneChip Genome-Wide Human SNP Cyto HD, following the protocol developed by the manufacturer (Affymetrix, Santa Clara, CA, USA). Data calculation was performed with Chromosome Analysis Suite 3.1.0.15 and NetAffx Build 33.1 (hg19).

Daunorubicin treatment

Fibroblasts were cultured as described above. The cells were cultured in T25 flasks to 80–90% confluence, then a non-lethal dose of 3 μM daunorubicin (Pfizer Pharma PFE GmbH, Berlin, Germany), was added. After two hours the medium was replaced 2, 4 h and 24 h post-treatment and the cells were harvested using trypsin. Quantification of γH2AX was performed as described previously [20].

Growth kinetics of FaDu and subclones

Tumor cell lines were cultured as described above. Cells were collected and seeded at a density of $5*10^4$ in T75 cell culture flasks in triplicates. The cells were harvested using trypsin and total cell numbers were determined using the Moxi^z automatic cell counter (Orflo, Ketchum, USA) at every time point. The cellular proliferation rate was calculated as the cumulative population doublings (CPD). The statistical analysis was done using the linear mixed-effects model fit by REML setting the biological replicate as a random variable.

Colony formation assay

Clonogenic survival was determined in colony formation assays adapted after Menegakis et al [21]. At passage p8, cells were seeded (1×10^5) in 10 cm diameter Petri dishes in triplicates. After five days and one medium change, the cells were irradiated with 2 Gy, 4 Gy, 6 Gy, and 8 Gy. Sham irradiated cells were kept at the same conditions in the radiation device control room (0 Gy). After 24 h cell suspensions were obtained for each dose and different seeding densities were plated in triplicates. Remaining cells were pelleted, washed with PBS and stored at -80 °C for further experiments. 14 days after irradiation colonies were fixed and stained with crystal violet. The image of a FaDu cell line (0 Gy) was made with the ZEISS Axiovert microscope using the Clone software at 10x magnification. The grayscale transformation was done with GIMP 2.10.14 software. Colonies defined as > 50 cells were counted and surviving fractions were expressed in terms of plating efficiency. Survival data after radiation were fitted to linear quadratic regression models employing the maximum likelihood approach (R package CFAssay). Differences between curves were evaluated using the F-test. Adjustment of p-values was done using the method of Benjamini and Hochberg.

Flow cytometry

Cells were washed with PBS (37 °C; 1 ml/25 cm^2) and trypsinized (Trypsin/EDTA (37 °C; 1 ml/ 25 cm^2), for 5 min at 37 °C. The reaction was stopped by the addition of a two-fold volume of culture medium at 37 °C and cells were collected by centrifugation at 300 x g for 6 min. 70% ethanol (-20 °C) was added dropwise to the cell pellet under permanent turbulence (~ 4 ml/10^5 cells) and the suspension was stored for ≥ 30 min at 4 °C or overnight. Later, the cell suspension was centrifuged at 300 x g for 6 min, and the supernatant was discarded. Cells were re-suspended in PBS (without magnesium and calcium -/-) with RNase (20 μg/ 10^4 cells) and incubated 30 min at 37 °C. After an additional centrifuge step of 300 x g for 6 min, cells were re-suspended in HOECHST 33258-staining solution (0.2 μg/ml in 1x PBS-/-) (~ 4 ml/ 10^5 cells) and again incubated for ≥ 30 min at 4 °C. The analysis was performed using FACS Canto II (BD Biosciences, Germany).

PCR and sequencing

Genomic DNA was isolated using the NucleoSpin tissue kit (Macherey-Nagel, Germany). PCR reactions were performed using the FastStart Taq DNA Polymerase, dNTPack, kit # 04738403001 (Roche Diagnostics, Germany). PCR was performed in three stages with one cycle of 5 min at 94 °C, forty cycles (15 sec, 94 °C, 30-sec primer TM, 1 min 68 °C) and one cycle of 2 min at 72 °C, using 30 ng DNA

per reaction. Primers were generated using, NCBI's (https://www.ncbi.nlm.nih.gov/tools/primer-blast/) primer designing tool. The following primer pairs were used; forward primer (AGGCAGTCAGTCGGAAAGTG) and reverse (TTGGAACCTGCTGATTCGCT) for *CHD2* (NM_001271) TM 62 °C; forward primer (ACAGCTGTTCTCACGGAAGG) and reverse (TAGGCTGCTGAGGATGGTCT) for *SPATA8* (NR_158221) TM 62 °C and forward primer (GCAAGAAGAAGATGAAGAGC) and reverse (GGCAGGTAAGCTCAGGTTTT) for *SMARCA1* (NM_003069) TM 64 °C. Sequence reactions were performed by Genterprise Germany, using PCR products digested with Exo/SaP (New England Biolabs, Germany).

Results

Epimutation screen of fibroblasts derived from childhood cancer patients using bisulfite pyrosequencing and deep bisulfite sequencing

In a previous study, we detected expression changes in tumor-related proteins as *RAD9A* in fibroblasts of former childhood tumor patients with the prevalent cancer types being leukemias and solid tumors [18]. Alteration of gene expression may be caused by methylation changes of promotor or other regulation sites. The methylation of tree CpG's in intron 2 of the *RAD9A* gene was proven to influence the expression of the RAD9A protein [22]. Therefore, we analyzed the methylation of intron 2 of the *RAD9A* gene and chose a panel of control genes (*APC, CDKN2A, EFNA5, TP53*) which were reported to be aberrantly methylated in related tumors and/or have a role in childhood malignancy (for further information see Supplementary references S3) using bisulfite pyrosequencing and deep bisulfite sequencing (DBS)

Bisulfite pyrosequencing. We have determined the mean methylation of the promoter regions in *APC* (NC_000084.6), *CDKN2A* (NC_000009.12), and *EFNA5* (NC_000005.10), a cis-regulatory region in *RAD9A* intron 2 (NC_000011.10), and a mutation hotspot in *TP53* exon 6 (NC_000017.11) in 20 primary fibroblast cell lines of cancer-free controls 0N and matched patients 1N and 2N (Fig. 1a-e). There were significant variations in methylation among the groups. *APC* (Fig. 1a) proved to be hypermethylated in 1N in comparison to the 0N control (adj.p-value = 0.03). *CDKN2A* (Fig. 1b), which is often mutated in a variety of cancers, exhibited hypermethylation in the 1N group (adj.p-value = 0.006) while it was hypomethylated in 2N group in comparison to 0N group (adj.p-value = 0.008). The 2N group showed a hypomethylation in *TP53* (Fig. 1c) in comparison to the control group 0N (adj.p-value = 0.01). No significant differences between the groups were detected for *RAD9A* genes (Fig. 1d) and *EFNA5* (Fig. 1e).

Outlier analysis. In previous work, we showed that outliers detected using bisulfit pyrosequencing could be considered as likely candidates for an abnormal methylation pattern, indicative of a mosaic epimutation [16]. So, we focused in this study on those cases. We identified three patients, one patient (1N08) who exhibited conspicuous hypermethylation (9%) of the *APC* promoter, another one (1N15) showed hypermethylation of *CDKN2A* (7%) and patient 2N12 displayed hypomethylation in *TP53* (95%). Five patients (1N04, 1N07, 1N14, 1N20, and 2N21) showed increased *RAD9A* intron 2 mean methylation, ranging from 10–31% (Fig. 1. a-d).

The average methylation changes could be due to either single CpG methylation errors at different positions in a large number of alleles or due to allele methylation errors, where most CpGs in individual DNA molecules are aberrantly methylated. Because it is usually the density of CpG methylation in a cis-regulatory region rather than individual CpGs that turns a gene "on" or "off" [23], allele methylation errors must be considered putatively as functionally relevant epimutations. To investigate the allele positions of the methylated CpG's we performed an analysis utilizing deep bisulfite sequencing (DBS).

Deep bisulfite sequencing can determine the methylation profiles of many thousands of individual DNA alleles for multiple genes and samples in a single experiment and thus directly measure epimutation rates (EMRs). To determine the density of CpGs and allele methylation ratio in the present study, we performed DBS on the patients with suspected epimutations (Table 1). Alleles with > 50% aberrantly (de)methylated CpGs in DBS are considered as functionally relevant epimutations. Consistent with an epimutation screen in breast cancer susceptibility genes [3], we considered EMRs > 1% as elevated and EMRs > 2.5% as likely pathogenic constitutive epimutations. Using the above-described classification, we did not detect any *APC* epimutations in fibroblasts of patient 1N08. Patient 1N15 displayed 0.2% EMRs in *CDKN2A* and patient 2N12 0.3% EMRs in *TP53*. Five patients with suspected *RAD9A* epimutations displayed 2.0–24.5% EMRs. Four childhood cancer patients (1N20, 1N14, 1N07 and 2N21) showed *RAD9A* epimutations and childhood cancer patient 1N04 showed an elevated *RAD9A* EMR. Overall, 10% (4 of 40) childhood cancer patients (1N and 2N) had *RAD9A* epimutations in their fibroblast cells (Table 1 and Fig. 1f).

Table 1
Results of methylation analysis (by bisulfite pyrosequencing and deep bisulfite sequencing) of patients with suspected epimutations

				bisulfite pyrosequencing		deep bisulfite sequencing			
Sample ID	First cancer*	Second cancer*	Gene harboring the putative epimutation	Mean (%) of all 1N and 2N patients	Mean (%) of the given patient	Mean (%) in a given patient	Alleles with > 60% methylation (%) EMR	Fully methylated alleles (%)	Fully unmethylated alleles (%)
1N08	ALL	-	*APC*	5	9	0.3	0	0	
1N15	ALL	-	*CDKN2A*	3	6.5	2.2	0.2	0	
2N12	Rhabdo-myosarcoma	Liver cancer	*TP53*	97	90	93			0.30
1N06 (control)	ALL	-	*RAD9A*	7	0	2.2	0.5	0.01	
1N04	Hodgkin lymphoma	-	*RAD9A*	7	13	9.3	2.0	0.3	
1N07	ALL	-	*RAD9A*	7	10	9,2	7.3	1.4	
1N14	Hodgkin lymphoma	-	*RAD9A*	7	14	12.6	5.9	0.7	
1N20	Retinoblastoma	-	*RAD9A*	7	31	32.3	24.5	11.5	
2N21	ALL	RA	*RAD9A*	7	12	10	3.2	0.9	
* ALL, acute lymphoblastic leukemia; RA, refractory anemia									
Supplementary Table S1: List of PCR- and sequencing primer for bisulfite pyrosequencing									

RAD9A **hypermethylation in the bone marrow of leukemia patients.**

Four childhood patients with *RAD9A* EMR > 2% suffered from leukemia. To corroborate the results of leukemic transformation, we analyzed firstly the methylation in the bone marrow of three leukemia patients. Patient P1 with pre-ALL and a Philadelphia chromosome in < 10% of analyzed (bone marrow) cells displayed a mean *RAD9A* methylation of 18%. Patient P2 with AML and 50% bone marrow cells with abnormal karyotype displayed a 29% *RAD9A* mean methylation whereas patient P3 with PBL and 60% cells of his bone marrow cells showed complex aberrations, consisting of a hypodiploid (28%) clone and a hyperdiploid line (32%), had a *RAD9A* mean methylation of 41% (Fig. 2a). Further analysis of bone marrow samples from 27 NHL and 26 AML patients revealed a *RAD9A* mean methylation of 30% for NHL and 20% for the AML patients ($p \leq 0.025$). We detected three NHL and four AML patients with elevated mean methylation. The values of the aberrant samples ranged from 38–66% for the NHL patients and from 14–63% for the AML patients (Fig. 2b). We were able to analyze several bone marrow samples taken in the course of therapy for three AML patients (Fig. 2c-e). The first bone marrow sample of AML patient 1 at diagnosis showed 36% mean hypermethylation of *RAD9A* intron 2 site. In course of the therapy, the methylation levels at first decreased (mean methylation 25%) but in the sample nr. 4 the mean methylation values raised again to 30% and shortly after this, the patient deceased (life period from diagnosis to death 19 months) (Fig. 2c). AML patient 2 had a rather high mean hypermethylation of 59% in the first bone marrow sample. Again, we could observe a slight decrease of methylation values (mean 44%) during the therapy, but one month later the values raised again (mean methylation 55%) and shortly after the last sample with the mean methylation value of 50% the patient deceased (life period from diagnosis to death was 4 months) (Fig. 2d). The first bone marrow sample of AML patient 3 displayed the mean methylation values of *RAD9A* of 27%. These values did slightly vary during the therapy. However in a short period of 2 months before the patient died, he displayed strong hypermethylation of 43%. This methylation further increased shortly before death to mean hypermethylation of 63% (life period from diagnosis to death was 27 months). To elucidate the reason for the increase of the methylation we analyzed bone marrow samples of this patient using genome-wide SNP array molecular karyotyping. As shown in Fig. 2e the analyzed samples display a progressive duplication of the 16p13.3(1,345,222-3,178,084) fragment in the last 2 months before death. The final duplicated region contains 106 genes of which 9 genes are known to be involved in cancer (*UBE2I, NUBP2, IGFALS, NTHL1, TSC2, PKD1, PDPK1, TCEB2, and TNFRSF12A*).

To substantiate the connection between alteration of important genes and the hypermethylation of *RAD9A*, we examined two primary fibroblast cell lines known to have homozygous mutations either in *BRCA2* (*FANCD1*) or in *SLX4* (*FANCP1*) in contrast to normal primary fibroblast cell lines (N = 20). As expected, fibroblast control cell lines exhibited *RAD9A* mean methylation values ranging from 3–11%, in contrast to *FANCD1* (28%) and *FANCP1* (47%).

RAD9A hypermethylation during EBV transformation and tumor development

According to Cheng and colleagues [22], *RAD9A* becomes an oncogene in breast cancer via hypermethylation in intron 2. This means if a cell becomes transformed to allow unlimited growth and show distinct tumor characteristics, changes in methylation values in intron 2 may be visible. Oncogenic transformation of B cells results in unlimited growth and has been associated with particular forms of cancer, such as Burkitt's lymphoma, Hodgkin's lymphoma, nasopharyngeal carcinoma, and gastric cancer. Thus, EBV infection is now widely used to generate immortal lymphoblastoid cell lines. Global changes in DNA methylation may contribute to the pathogenesis of EBV [24]. We, therefore, tested EBV transformed lymphoblasts for changes in methylation of *RAD9A* in intron 2 using bisulfit sequencing. The mean methylation varied in six different EBV transformed cell lines from 6–41% (Fig. 3a). The DBS analysis of the cell line with the highest mean methylation value exhibited 9% fully methylated alleles (the corresponding fibroblast cell line showed 8% mean methylation in *RAD9A*). In contrast, the methylation patterns of *APC*, *BRCA1*, *CDKN2A*, and *TP53* remained virtually unchanged in this cell line after EBV transformation (Fig. 3b).

RAD9A hypermethylation in tumor cell lines and FaDu subclones

Tumor cell lines. To understand the role of hypermethylation of *RAD9A* in cancer and oncogenic transformation, we analyzed BT-549 (breast cancer), MCF7 (breast cancer), EFO-21 (ovary), T47D (breast cancer), and FaDu (squamous cell carcinoma) cell lines. The hypermethylation varied between these tumor cell lines (mean values 20–81%, Fig. 4a). The highest methylation in all three CpG's was detected in the cell line EFO-21 of CpG1-84%, CpG2-89%, and CpG3-76%. The methylation values seem to be independent of the *RAD9A* copy number. The MCF7 cell line (mean methylation 24%) has two copies of Chr.11 and one derivative (der(?)t(11;1;17;19;17)), in contrast to EFO-21 (mean methylation 83%) and FaDu cell line (mean methylation 54%) with up to three copies of chromosome 11.

FaDu subclones. If *RAD9A* methylation is relevant for tumor development and is not due to changed chromosomal numbers but gene alteration, it should be possible to detect divergent methylation in tumor subclones. Subclonal events with gene mutations were reported by Nisar et al. 2016 and recently by Ben-David et al. 2018 with the consequence of copy number gains and losses and consequently different drug responses [25, 26]. To test the hypothesis that subclonal events may be responsible for methylation changes in *RAD9A* we established several subclones of the FaDu cell line. The FaDu cell line exhibits homozygous loss of function mutations in *TP53* and *CDKN2A* genes, therefore, chromosomal changes caused by the lack of proper DNA repair may occur frequently. During the cultivation of the parental FaDu cell line, subclonal events lead to a certain number of divergent cells (Fig. 4b). We were able to generate thirteen subclonal cell lines with divergent *RAD9A* methylation patterns (Fig. 4c). Two of the subclones, 4 and 6, exhibit high *RAD9A* methylation values (mean methylation 75% and 73% respectively) in comparison to the parental cell line (mean methylation 54%), while others showed a lower methylation level (e.g. subclone 2; mean 42% and subclone 9; mean 40%). The methylation levels of *RAD9A* remained stable during cultivation for all clones. Clones 2, 4, 6, 9 and 10 and the parental FaDu cell line were chosen for further characterization.

Subclone characterization. Monolayer culture growth kinetics, for the subclones 2, 4, 9 and the parental FaDu cell line using triplicates revealed significantly delayed growth for subclone 4 (p-value < 0.0001) (Fig. 4d). Clonogenic survival experiments upon irradiation performed with the subclones 2, 4, 9 and the FaDu cell line resulted in significantly reduced survival of the clone 4 (adj p-value. <0.0003) and clone 2 (adj p-value < 0.001) in comparison to the FaDu parental cell line (Fig. 4e, f). Methylation signatures for the clones in clonogenic survival experiments matched the untreated clone signatures.

SNP array analysis provides a more detailed view of chromosomal alterations. Using this technique, we analyzed subclones with hypermethylation (4, 6 and 10) in comparison to low methylation (subclones 2 and 9) and the parental FaDu cell line. The obtained karyograms matched the karyogram of the FaDu parental cell line. No structural chromosomal differences between the analyzed subclones and parental cell line could be detected; instead, we identified a homozygous deletion in 15q26.1q26.2 unique to subclone 4 and a heterozygous deletion in Xq25 in subclone 6. Downstream analysis using PCR and Sanger sequencing confirmed the homozygous deletion of the *CHD2* and *SPATA8* genes in subclone 4 and the stop codon mutation c.537 538insG, p.P182fs*18 in the remaining allele of *SMARCA1* (*SNF2L*) gene in subclone 6. Both genes harbor a helicase domain and are involved in DNA-repair and transcription regulation [27, 28] (Fig. 5a and b).

In contrast to the subclones 4, 6, and FaDu, the subclone 10 displayed a 302 kb duplication in 16q23.1(75,318,494 – 75,620,953). The duplication encompasses 6 genes of which 4 are frequently deregulated in cancer (*TMEM170A, CHST6, CHST5, TMEM231*). The *TMEM231* gene is responsible for the Joubert Syndrome 20; (OMIM 614970) and the *GABARAPL2* is involved in the autophagy interaction network (Fig. 5c).

Effects of radiation and chemotherapeutics on RAD9A **methylation**

As most of our patients (except patient 1N20) did receive chemo- and radiotherapy following diagnosis and the donation of the fibroblasts was done in adulthood, several years after the first malignancy, we designed experiments that may clarify whether treatment of the malignancies has an impact on the methylation of *RAD9A* or if *RAD9A*-methylation is a potential stable methylation marker.

Effects of radiation. We have previously shown that DNA methylation remains relatively stable in primary fibroblasts throughout the first cell cycle after irradiation [29]. In contrast, significant methylation changes in > 250 genes and the MAP kinase signaling pathway were associated with delayed radiation effects in single-cell clones of irradiated fibroblast [30]. To study radiation effects on the mean methylation of the *RAD9A* intron 2 site, the control cell line 0N18 was analyzed at 15 min, 2 and 24 h after irradiation with 0 Gy, 2 Gy, 5 Gy, and 8 Gy at each time point. The *RAD9A* mean methylation values in intron 2 remained virtually unchanged between 7% and 9% (Fig. 6a). As *RAD9A* expression is deregulated in a variety of tumors and plays an important role in DNA repair, we additionally performed experiments with three fibroblast strains (1N08, 0N12, and 2N12) which were irradiated in fractions of 8 × 2 Gy, 4 × 4 Gy, 8 × 4 Gy, 10 × 2 Gy, and 10 × 4 Gy within 20 days. Again, *RAD9A* mean methylation remained rather constant at 5% in 1N08 and 2N12, and at 8–9% in 0N12 cell lines (Fig. 6b). Furthermore, we performed experiments in exponentially growing FaDu tumor cells to estimate the mean methylation values of *RAD9A*. The cells were analyzed at 2, 4, and 24 h after irradiation with a single dose of 0 Gy, 2 Gy, 5 Gy, and 8 Gy. The *RAD9A* mean methylation varied within a narrow range of 54–57% and there was no difference between irradiated and non-irradiated cells (Fig. 6c). The proportion of G2-phase cells (measured by flow cytometry for FaDu cells) increased with radiation dose and time after irradiation, ranging from 35% G2-phase cells in non-irradiated cells to 65% at 24 h after 8 Gy indicating a functional G2/M checkpoint (Fig. 6d).

Effects of chemotherapeutics. Although tumor therapy varied between patients, daunorubicin and doxorubicin were frequently used in the treatment regimens. As both drugs have similar properties and the cellular uptake of daunorubicin is superior to that of doxorubicin, we analyzed the influence of daunorubicin on *RAD9A* methylation. Treatment of normal fibroblasts with 3 µM daunorubicin, as stated in the study of Przybylska et al. [31], yields a surviving cell fraction of 60%. Analysis of γH2AX as a marker for DNA double-strand breaks confirmed the incorporation and toxicity of daunorubicin in the cells (Fig. 6e). Examination of the methylation signature at 0, 1, 4, 12 and 24 h post-treatment showed no significant changes in methylation in two independent fibroblast cell lines. The 2N24 cell line exhibited mean methylation values of 4–6% and 0N24 control cell line of 9–12% (Fig. 6f).

Discussion

RAD9A methylation in childhood cancer patients. The vast majority of childhood cancers occur sporadically and cannot be explained by inherited mutations in known tumor susceptibility genes [8]. Therefore, it seems plausible to assume that stochastic or adverse exposure event during early (intrauterine and postnatal) development increase cancer susceptibility through epigenetic reprogramming [11, 32]. Consistent with the developmental programming of cancer hypothesis, we previously identified a monozygotic twin pair, discordant for childhood cancer with a constitutive *BRCA1* epimutation in the twin with cancer [16]. In a previous study, we detected reduced expression levels of RAD9A in primary fibroblast cells of childhood cancer patients with a second primary tumor, suggests a function of *RAD9A* as a genomic caretaker [18]. The *RAD9A* gene is involved in different DNA repair pathways, including base excision repair, homologous recombination, and mismatch repair, alongside multiple cell cycle phase checkpoints and apoptosis [33]. The methylation of tree CpG's in intron 2 of the *RAD9A* gene was proven to influence the expression of the RAD9A protein [22], therefore, we performed a DNA methylation analysis in *RAD9A* in primary fibroblasts of matched childhood cancer patients and controls aiming to detect aberrant constitutive or mosaic methylation patterns including a panel of control genes consisting of *APC*, *CDKN2A*, *EFNA5, TP35* (for further information see supplementary references S3). Although we detected 1–2% changes in methylation values in *APC*, *CDKN2A* and *TP53* gene, it is questionable if these low variances in methylation may have biological significance. The lack of significant allele methylation values in the 1N08 (*APC*), 1N15 (*CDKN2A*) and 2N12 (*TP53*) patients substantiate our assumption further.

We did not detect significant methylation changes in *EFNA5* and *RAD9A* in fibroblasts of former childhood cancer patients but we identified 5 patients with ≥10% mean *RAD9A* methylation and ≥2% hypermethylated alleles. Previously, we have shown that epimutations in *BRCA1* and *RAD51* can originate in single precursor cells [3, 34]. It is, therefore, difficult to define a threshold for

constitutive epimutations in normal tissues that can be associated with tumor formation. In our experience with screening for TS epimutations in more than 800 individuals [3, 34], mean methylation values of ≥10% and allele methylation errors of ≥2–3% (depending on the gene and assay) are outside the normal methylation variation range (depending on the tissue origin analyzed). The error rate for copying DNA methylation patterns during DNA replication is estimated to be 10–100 times higher than for non-replicating DNA [14, 35]. Therefore, rapidly dividing cells, e.g. stem cells during embryonal development and organogenesis, may be particularly vulnerable for acquiring methylation defects [10, 36]. Patient 1N20, who suffered from sporadic unilateral retinoblastoma, exhibited almost 12% fully methylated *RAD9A* alleles in fibroblasts, indicating that almost one-eighth of his normal cells are endowed with epimutated *RAD9A* alleles. Most retinoblastomas, which are derived from the cone photoreceptor lineage, show biallelic inactivation of the *RB1* tumor suppressor gene, but additional (epi)genetic changes are most likely required for tumor development. A small subset (1–2%) of unilateral tumors without *RB1* mutations are characterized by high-level amplification of the *MYCN* oncogene. We did not detect an *RB1* germline mutation in our retinoblastoma patient, however, the mutational status of the tumor is not known. Instead, we detected a unique mosaic duplication in 13q14.3 including the genes *CKAP2*, *THSD1* and *VPS36* in the patient's fibroblasts. The *CKAP2* gene is a cytoskeleton-associated protein that stabilizes microtubules and plays a role in the regulation of cell division [37]. Whether this gene alteration contributes to the development of this individual sporadic retinoblastoma has to be elucidated but this gene copy alteration could be associated with the described hypermethylation in *RAD9A* in this patient. The unusually high rate of abnormally methylated *RAD9A* alleles in our patient indicates that *RAD9A* epimutations could mechanistically contribute to retinoblastoma development. The retinoblastoma was cured solely by excision of the tumor; therefore, no therapy-related changes may be expected. Constitutive epimutations (allele methylation errors) that arise in early development are likely to be present in a mosaic state in different tissues of an individual. Nevertheless, the risk for malignant transformations may increase with the percentage of cells with compromised genomic caretakers. When the analyzed childhood cancer patients were recruited for this study, they all had survived an initial cancer treatment (in most cases including radiation therapy) and the 2N patients had been tumor-free for several years. Although we did not find evidence for irradiation or chemotherapy-induced *RAD9A* epimutations, we cannot completely exclude the possibility that the observed *RAD9A* hypermethylation in some patients is a consequence of cancer treatment which leads to mutation of important genes. Since all patients were analyzed using a genome-wide SNP array and no variants in *RAD9A* or neighboring genes were detected, the possibility of methylation changes due to genetic (allelic) variants seems unlikely. Studies suggest that methylation may change during lifetime [38]. Since the childhood cancer patients and controls enrolled in this study were age-matched we can assume that the methylation values are comparable and are not affected by age factors in this cohort.

The other four patients with ≥2% hypermethylated alleles in *RAD9A* suffered from leukemia. Because to date, there is no research about the involvement of *RAD9A* hypermethylation and leukemia development and progression we designed experiments with EBV, tumor cell lines, and bone marrow samples from leukemia patients to elucidate a possible mechanistic involvement.

RAD9A hypermethylation in leukemia. In our experiments the EBV transformation of resting B cells to proliferating lymphoblasts induced dramatic variation in *RAD9A* methylation, indicating that epigenetic dysregulation of *RAD9A* may occur during malignant transformation early in tumorigenesis. The involvement of *RAD9A* hypermethylation in oncogenic transformation is further substantiated with experiments performed with bone marrow samples from leukemia patients, analysis of Fanconi fibroblasts and the generation and examination of subclones derived from the FaDu tumor cell line. To our knowledge, this study is the first analysis of *RAD9A* methylation in bone marrow samples taken during the therapy of leukemia.

The intron 2 hypermethylation, which is consistent with an oncogenic function was found in breast- and prostate cancer [22, 44]. More than 45% of prostate tumors have aberrantly high levels of RAD9A. It has been previously shown that hypermethylation of *RAD9A* intron 2 is associated with mRNA and protein overexpression, which may be a critical step in the development of prostate and breast cancer [44, 45]. Decreased RAD9A abundance mediated by RNA interference in prostate cancer cell lines dramatically reduces tumorigenicity in nude mouse xenographs, indicating that RAD9A has a critical, causal role in this type of cancer [44].

We could detect a significant change in methylation values of *RAD9A* between AML and NHL patients. Moreover, we could show an evolving duplication on chr.16p13.3, including genes that could be responsible for the hypermethylation of *RAD9A* and the progression of AML. One of the duplicated genes is *NTHL1*. Its overexpression causes genomic instability and loss of contact inhibition of cells [39]. Another duplicated gene in chr.16p13.3 is *PRKD1*. High *PRKD1* mRNA levels have been associated with low overall survival in TNBC (triple-negative breast cancer) [40]. *TNFRS12A*, also located in the 16p13.3 duplication, is responsible for poor prognosis in breast cancer, if overexpressed [41]. Although the results indicate some tumor-related methylation values of *RAD9A*, the relationship between tumor type, survival and *RAD9A* hypermethylation demands larger patients studies.

Fanconi fibroblasts are derived from patients with rare genetic diseases resulting in impaired response to DNA damage. Among those affected, the majority develop cancer, most often acute myelogenous leukemia, and 90% develop bone marrow failure. We detected in comparison to unaffected fibroblasts an hypermethaltion of the *RAD9A* gene in Fanconi fibroblasts which further confirms our assumption of a possible involvement of *RAD9A* in tumor formation. The experiments in generated subclones of FaDu cell line show a dynamic evolvement of different tumor subpopulations and consequently different *RAD9A* methylation values in each subclone. The role of *RAD9A* for the cell fate and possible therapy outcome needs to be investigated in more detail. The hitherto existing findings suggest a connection between chromosomal integrity, pathogenic alteration of crucial genes and hypermethylation of the *RAD9A* locus.

A possible mechanistic model of RAD9A regulation. RAD9A forms the RAD9A-HUS1-RAD1 complex and is recruited to sites of DNA damage and required for cell cycle arrest and DNA damage repair [42]. When translocated to mitochondria, RAD9A binds and neutralizes the anti-apoptotic activity of BCL-2 and BCL-xL proteins, thus promoting cell death [43]. However, permanent RAD9A overexpression may also have harmful, tumor-promoting effects, disturbing the correct DNA repair. On the other hand, the hypermethylation of the intron 2 site could also be an apoptotic signal, indicating critical damage in other genes. The methylation-sensitive region in intron 2 of *RAD9A* is endowed with three regulatory elements, annotated in ORegAnno (http://www.oreganno.org/). Element OREG1137234 is a binding site for the transcription factor *ZNF263*, which functions as a transcriptional repressor. It is plausible to assume that intron 2 hypermethylation interferes with ZNF263 binding, which then activates RAD9A expression.

Conclusion

Aberrant methylation and the reasons and consequences of this change in cancer types other than breast and prostate cancer have to be elucidated yet. According to the Cancer Genome Atlas/TCGA (https://cancergenome.nih.gov/), *RAD9A* is overexpressed in a wide variety of tumors including leukemia and solid tumors, supporting further its oncogenic function. Our experiments with EBV transformed lymphoblasts, the FaDu squamous cell carcinoma cell line and leukemia tumor samples may point towards a broad spectrum of tumor entities with an aberrant methylation of *RAD9A* and the use *RAD9A* methylation values as a candidate biomarker as suggested for prostate cancer [46]. We found significant differences in *RAD9A* methylation between AML and NHL patients and selected bone marrow samples during therapy, suggesting the possibility to use *RAD9A* methylation as a therapeutic marker in leukemia and childhood cancer. However additional trials must be conducted to prove this approach. We propose that *RAD9A* methylation can be an early (either stochastic or environmentally induced) event, which may increase the probability of malignant transformation in body cells (predisposing factor) or/and a factor that promotes the tumor progression itself (oncogenic factor). We are aware that the patients presented here, were selected based on survival criteria. Therefore, larger prospective studies in various cancer types and tissues are needed to generally correlate *RAD9A* epimutations with cancer incidence and therapy outcomes.

Abbreviations

TS–tumor suppressor, HNPCC–hereditary non-polyposis colon cancer, EBV–Epstein Barr virus, B-ALL–acute lymphocytic leukemia, AML–Acute myeloid leukemia, PBL–plasmablastic lymphoma, CAF–cancer-associated fibroblasts, FANC–Fanconi anemia, FACS–flow cytometric cell cycle, DMEM–Dulbecco's modified Eagle's medium, FBS–fetal bovine serum, EMRs–epimutation rates, DBS–deep bisulfite sequencing, Gy–Gray, RA–refractory anemia,

Declarations

Ethics approval and consent to participate

Participants were informed in writing and verbally of the procedures and purpose of this study. Signed informed consent documents were obtained from both patients and healthy individuals. Study protocols were approved by the Ethics Committee of the Medical Association of Rhineland-Palatinate (no. 837.440.03 [4102], 837.103.04 [4261], 837.262.12 [8363-F] and no. 2019-14677). All the subsequent research analyses were carried out in accordance with the approved guidelines and regulations.

Consent for publication

Not applicable

Availability of data and materials

The datasets generated and analyzed during the current study are not publicly available due to ethic and data protection reasons but are available from the corresponding author on reasonable request.

Competing interests

The authors declare no conflict of interest

Funding

This study was supported by The BMBF German ministry for education and science [02NUK016A, 02NUK042A, 2NUK042B and 2NUK042C]

Authors' contributions

D.G. and **J.B** contributed equally to this work, and should be considered co-first authors, **MD** analyzed the bNGS data. **DG, OS, ML**, **JM,** prepared cell culture radiation and pyrosequencing experiments. **MR** and **WB** prepared the tumor cell lines and bone marrow samples. **MLI** and **DG** conducted the SNP array molecular karyotyping. **HR** helped with the analysis of pyro sequence data. **JB** and **OS** prepared the bisulfite sequence bNGS and provided the data interpretation. C**S, MM**, organized the patient's recruitment. **DG, TH, DP** and **SH** conceived and designed this project and wrote the paper. All authors revised the manuscript critically for important intellectual content and approved the final version and agreed to be accountable for all aspects of the work in ensuring that questions related to the accuracy or integrity of any part of the work are appropriately investigated and resolved.

Acknowledgments

First of all, we would like to thank the patients for participating in this study. Our clinical staff also deserves special thanks. We also thank Ursula Dique-Kaiser, Britta Weber, Danuta Wieczorek, Martina Mihm, Brigitte Schuh and Martina Hermanns for technical support. We kindly thank Prof. Detlev Schindler for the donation of Fanconi Fibroblasts. We are grateful to Benjamin Irmscher for providing the daunorubicin experiments. Special thanks to Heather Chorzempa for the proofreading of this manuscript.

References

1. Karakosta A, Golias C, Charalabopoulos A, Peschos D, Batistatou A, Charalabopoulos K. Genetic models of human cancer as a multistep process. Paradigm models of colorectal cancer, breast cancer, and chronic myelogenous and acute lymphoblastic leukaemia. J Exp Clin Cancer Res. 2005;24:505–14.
2. Ting AH, McGarvey KM, Baylin SB. The cancer epigenome–components and functional correlates. Genes Dev. 2006;20:3215–31. doi:10.1101/gad.1464906.
3. Böck J, Appenzeller S, Haertle L, Schneider T, Gehrig A, Schröder J, et al. Single CpG hypermethylation, allele methylation errors, and decreased expression of multiple tumor suppressor genes in normal body cells of mutation-negative early-onset and high-risk breast cancer patients. Int J Cancer. 2018;143:1416–25. doi:10.1002/ijc.31526.
4. Goel A, Nguyen T-P, Leung H-CE, Nagasaka T, Rhees J, Hotchkiss E, et al. De novo constitutional MLH1 epimutations confer early-onset colorectal cancer in two new sporadic Lynch syndrome cases, with derivation of the epimutation on the paternal allele in one. Int J Cancer. 2011;128:869–78. doi:10.1002/ijc.25422.
5. Hitchins MP. Finding the needle in a haystack: identification of cases of Lynch syndrome with MLH1 epimutation. Fam Cancer. 2016;15:413–22. doi:10.1007/s10689-016-9887-3.
6. Ligtenberg MJL, Kuiper RP, Chan TL, Goossens M, Hebeda KM, Voorendt M, et al. Heritable somatic methylation and inactivation of MSH2 in families with Lynch syndrome due to deletion of the 3' exons of TACSTD1. Nat Genet. 2009;41:112–7. doi:10.1038/ng.283.

7. Raval A, Tanner SM, Byrd JC, Angerman EB, Perko JD, Chen S-S, et al. Downregulation of death-associated protein kinase 1 (DAPK1) in chronic lymphocytic leukemia. Cell. 2007;129:879–90. doi:10.1016/j.cell.2007.03.043.
8. D'Orazio JA. Inherited cancer syndromes in children and young adults. J Pediatr Hematol Oncol. 2010;32:195–228. doi:10.1097/MPH.0b013e3181ced34c.
9. van Echten-Arends J, Mastenbroek S, Sikkema-Raddatz B, Korevaar JC, Heineman MJ, van der Veen F, Repping S. Chromosomal mosaicism in human preimplantation embryos: a systematic review. Hum Reprod Update. 2011;17:620–7. doi:10.1093/humupd/dmr014.
10. Tomasetti C, Li L, Vogelstein B. Stem cell divisions, somatic mutations, cancer etiology, and cancer prevention. Science. 2017;355:1330–4. doi:10.1126/science.aaf9011.
11. Marshall GM, Carter DR, Cheung BB, Liu T, Mateos MK, Meyerowitz JG, Weiss WA. The prenatal origins of cancer. Nat Rev Cancer. 2014;14:277–89. doi:10.1038/nrc3679.
12. McHale CM, Wiemels JL, Zhang L, Ma X, Buffler PA, Feusner J, et al. Prenatal origin of childhood acute myeloid leukemias harboring chromosomal rearrangements t(15;17) and inv(16). Blood. 2003;101:4640–1. doi:10.1182/blood-2003-01-0313.
13. Gale KB, Ford AM, Repp R, Borkhardt A, Keller C, Eden OB, Greaves MF. Backtracking leukemia to birth: Identification of clonotypic gene fusion sequences in neonatal blood spots. Proc Natl Acad Sci U S A. 1997;94:13950–4.
14. Bennett-Baker PE, Wilkowski J, Burke DT. Age-associated activation of epigenetically repressed genes in the mouse. Genetics. 2003;165:2055–62.
15. Lønning PE, Eikesdal HP, Løes IM, Knappskog S. Constitutional Mosaic Epimutations - a hidden cause of cancer? Cell Stress. 2019;3:118–35. doi:10.15698/cst2019.04.183.
16. Galetzka D, Hansmann T, El Hajj N, Weis E, Irmscher B, Ludwig M, et al. Monozygotic twins discordant for constitutive BRCA1 promoter methylation, childhood cancer and secondary cancer. Epigenetics. 2012;7:47–54. doi:10.4161/epi.7.1.18814.
17. Etzold A, Galetzka D, Weis E, Bartsch O, Haaf T, Spix C, et al. CAF-like state in primary skin fibroblasts with constitutional BRCA1 epimutation sheds new light on tumor suppressor deficiency-related changes in healthy tissue. Epigenetics. 2016;11:120–31. doi:10.1080/15592294.2016.1140295.
18. Weis E, Schoen H, Victor A, Spix C, Ludwig M, Schneider-Raetzke B, et al. Reduced mRNA and protein expression of the genomic caretaker RAD9A in primary fibroblasts of individuals with childhood and independent second cancer. PLoS ONE. 2011;6:e25750. doi:10.1371/journal.pone.0025750.
19. Automated methylation analysis of amplicons from bisulfite flowgram sequencing
Rahmann S, Beygo J, Kanber D, Martin M, Horsthemke B, Buiting K. Amplikyzer. Automated methylation analysis of amplicons from bisulfite flowgram sequencing; 2013.
20. Weis E, Galetzka D, Herlyn H, Schneider E, Haaf T. Humans and chimpanzees differ in their cellular response to DNA damage and non-coding sequence elements of DNA repair-associated genes. Cytogenet Genome Res. 2008;122:92–102. doi:10.1159/000163086.
21. Menegakis A, Yaromina A, Eicheler W, Dörfler A, Beuthien-Baumann B, Thames HD, et al. Prediction of clonogenic cell survival curves based on the number of residual DNA double strand breaks measured by gammaH2AX staining. Int J Radiat Biol. 2009;85:1032–41. doi:10.3109/09553000903242149.
22. Cheng CK, Chow LWC, Loo WTY, Chan TK, Chan V. The cell cycle checkpoint gene Rad9 is a novel oncogene activated by 11q13 amplification and DNA methylation in breast cancer. Cancer Res. 2005;65:8646–54. doi:10.1158/0008-5472.CAN-04-4243.
23. Weber M, Hellmann I, Stadler MB, Ramos L, Pääbo S, Rebhan M, Schübeler D. Distribution, silencing potential and evolutionary impact of promoter DNA methylation in the human genome. Nat Genet. 2007;39:457–66. doi:10.1038/ng1990.
24. Hernandez-Vargas H, Gruffat H, Cros MP, Diederichs A, Sirand C, Vargas-Ayala RC, et al. Viral driven epigenetic events alter the expression of cancer-related genes in Epstein-Barr-virus naturally infected Burkitt lymphoma cell lines. Sci Rep. 2017;7:5852. doi:10.1038/s41598-017-05713-2.
25. Amin NA, Seymour E, Saiya-Cork K, Parkin B, Shedden K, Malek SN. A Quantitative Analysis of Subclonal and Clonal Gene Mutations before and after Therapy in Chronic Lymphocytic Leukemia. Clin Cancer Res. 2016;22:4525–35. doi:10.1158/1078-0432.CCR-15-3103.
26. Ben-David U, Siranosian B, Ha G, Tang H, Oren Y, Hinohara K, et al. Genetic and transcriptional evolution alters cancer cell line drug response. Nature. 2018;560:325–30. doi:10.1038/s41586-018-0409-3.
27. Luijsterburg MS, Krijger I de, Wiegant WW, Shah RG, Smeenk G, Groot AJL de, et al. PARP1 Links CHD2-Mediated Chromatin Expansion and H3.3 Deposition to DNA Repair by Non-homologous End-Joining. Mol Cell. 2016;61:547–62.

doi:10.1016/j.molcel.2016.01.019.

28. Eckey M, Kuphal S, Straub T, Rümmele P, Kremmer E, Bosserhoff AK, Becker PB. Nucleosome remodeler SNF2L suppresses cell proliferation and migration and attenuates Wnt signaling. Mol Cell Biol. 2012;32:2359–71. doi:10.1128/MCB.06619-11.
29. Maierhofer A, Flunkert J, Dittrich M, Müller T, Schindler D, Nanda I, Haaf T. Analysis of global DNA methylation changes in primary human fibroblasts in the early phase following X-ray irradiation. PLoS ONE. 2017;12:e0177442. doi:10.1371/journal.pone.0177442.
30. Flunkert J, Maierhofer A, Dittrich M, Müller T, Horvath S, Nanda I, Haaf T. Genetic and epigenetic changes in clonal descendants of irradiated human fibroblasts. Exp Cell Res. 2018;370:322–32. doi:10.1016/j.yexcr.2018.06.034.
31. Przybylska M, Koceva-Chyla A, Rózga B, Józwiak Z. Cytotoxicity of daunorubicin in trisomic (+ 21) human fibroblasts: relation to drug uptake and cell membrane fluidity. Cell Biol Int. 2001;25:157–70. doi:10.1006/cbir.2000.0583.
32. Walker CL, Ho S-m. Developmental reprogramming of cancer susceptibility. Nat Rev Cancer. 2012;12:479–86. doi:10.1038/nrc3220.
33. Lieberman HB, Bernstock JD, Broustas CG, Hopkins KM, Leloup C, Zhu A. The role of RAD9 in tumorigenesis. J Mol Cell Biol. 2011;3:39–43. doi:10.1093/jmcb/mjq039.
34. Hansmann T, Pliushch G, Leubner M, Kroll P, Endt D, Gehrig A, et al. Constitutive promoter methylation of BRCA1 and RAD51C in patients with familial ovarian cancer and early-onset sporadic breast cancer. Hum Mol Genet. 2012;21:4669–79. doi:10.1093/hmg/dds308.
35. Horsthemke B. Epimutations in human disease. Curr Top Microbiol Immunol. 2006;310:45–59.
36. Lopez-Lazaro M. The stem cell division theory of cancer. Crit Rev Oncol Hematol. 2018;123:95–113. doi:10.1016/j.critrevonc.2018.01.010.
37. Yoo BH, Park C-H, Kim H-J, Kang D-S, Bae C-D. CKAP2 is necessary to ensure the faithful spindle bipolarity in a dividing diploid hepatocyte. Biochem Biophys Res Commun. 2016;473:886–93. doi:10.1016/j.bbrc.2016.03.145.
38. Horvath S, Raj K. DNA methylation-based biomarkers and the epigenetic clock theory of ageing. Nat Rev Genet. 2018;19:371–84. doi:10.1038/s41576-018-0004-3.
39. Limpose KL, Trego KS, Li Z, Leung SW, Sarker AH, Shah JA, et al. Overexpression of the base excision repair NTHL1 glycosylase causes genomic instability and early cellular hallmarks of cancer. Nucleic Acids Res. 2018;46:4515–32. doi:10.1093/nar/gky162.
40. Spasojevic C, Marangoni E, Vacher S, Assayag F, Meseure D, Château-Joubert S, et al. PKD1 is a potential biomarker and therapeutic target in triple-negative breast cancer. Oncotarget. 2018;9.
41. Yang J, Min K-W, Kim D-H, Son BK, Moon KM, Wi YC, et al. High TNFRSF12A level associated with MMP-9 overexpression is linked to poor prognosis in breast cancer: Gene set enrichment analysis and validation in large-scale cohorts. PLoS ONE. 2018;13:e0202113. doi:10.1371/journal.pone.0202113.
42. Tsai F-L, Kai M. The checkpoint clamp protein Rad9 facilitates DNA-end resection and prevents alternative non-homologous end joining. Cell Cycle. 2014;13:3460–4. doi:10.4161/15384101.2014.958386.
43. Yoshida K, Komatsu K, Wang H-G, Kufe D. c-Abl Tyrosine Kinase Regulates the Human Rad9 Checkpoint Protein in Response to DNA Damage. Mol Cell Biol. 2002;22:3292–300. doi:10.1128/MCB.22.10.3292-3300.2002.
44. Zhu A, Zhang CX, Lieberman HB. Rad9 has a functional role in human prostate carcinogenesis. Cancer Res. 2008;68:1267–74. doi:10.1158/0008-5472.CAN-07-2304.
45. Broustas CG, Zhu A, Lieberman HB. Rad9 protein contributes to prostate tumor progression by promoting cell migration and anoikis resistance. J Biol Chem. 2012;287:41324–33. doi:10.1074/jbc.M112.402784.
46. Lieberman HB, Rai AJ, Friedman RA, Hopkins KM, Broustas CG. Prostate cancer: unmet clinical needs and RAD9 as a candidate biomarker for patient management. Transl Cancer Res. 2018;7:651–61. doi:10.21037/tcr.2018.01.21.

Description Of Supplementary Files

Supplementary Table S1. List of PCR- and sequencing primer for bisulfite pyrosequencing.

Supplementary Table S2.

Primers for deep bisulfite sequencing.

Supplementary references S3

Figures

Fig. 1

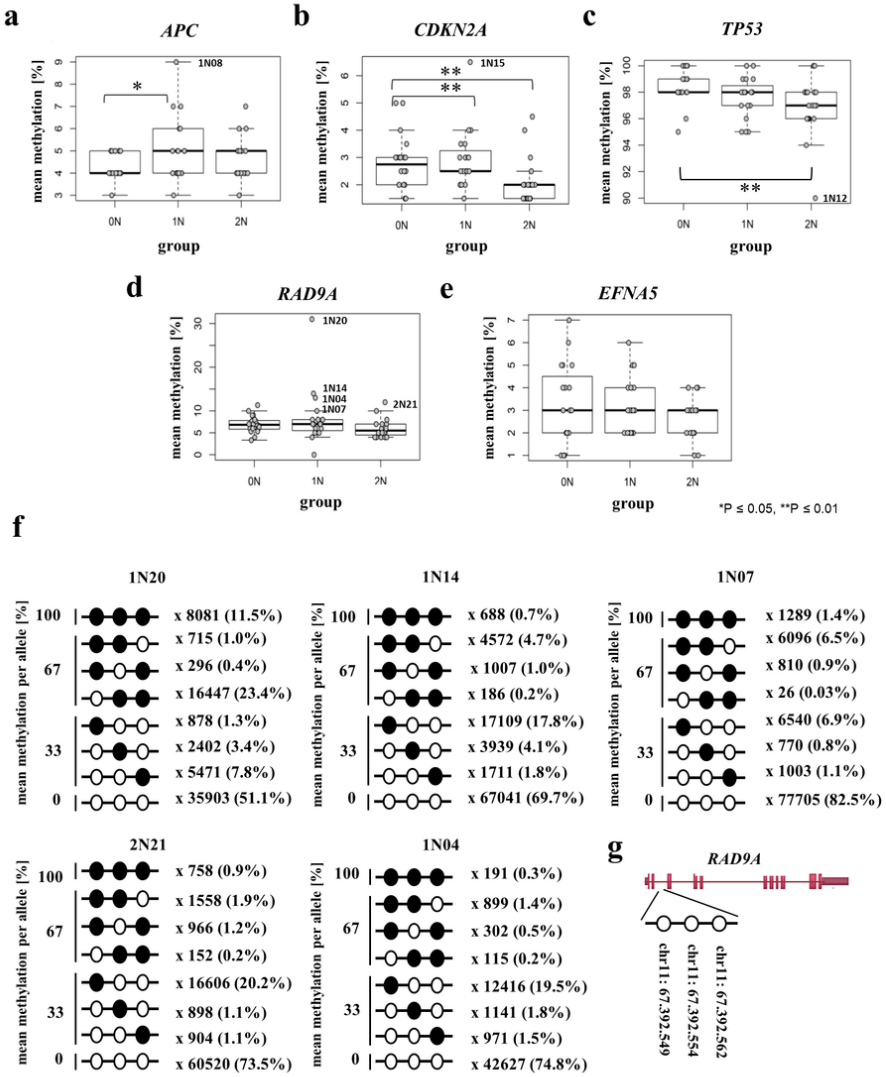

Figure 1

Methylation analysis of candidate genes and deep bisulfite sequencing analysis of RAD9A. Box plots show the distribution of (a) APC, (b) CDKN2A, (c) TP53, (d) RAD9A and (e) EFNA methylation values in 20 healthy controls (0N), 20 one-cancer (1N), and 20 two-cancer (2N) patients including outliers which are also listed in Table 1. The bottom and the top of the boxes represent the 25th and 75th percentiles, respectively. The median is represented by a vertical line. Bars extend from the boxes to at most 1.5 times the height of the box. Statistical comparison was performed using the Kruskal-Wallis rank-sum test. *P ≤ 0.05, **P ≤ 0.01. (f) Four 1N (1N20, 1N14, 1N07, 1N04) and one 2N (2N21) patient were analyzed using deep bisulfite sequencing and the results of RAD9A allele mean methylation values are shown in lollipop diagrams for each patient. (g) Position of CpG1-3 in RAD9A on chromosome 11.

Fig. 2

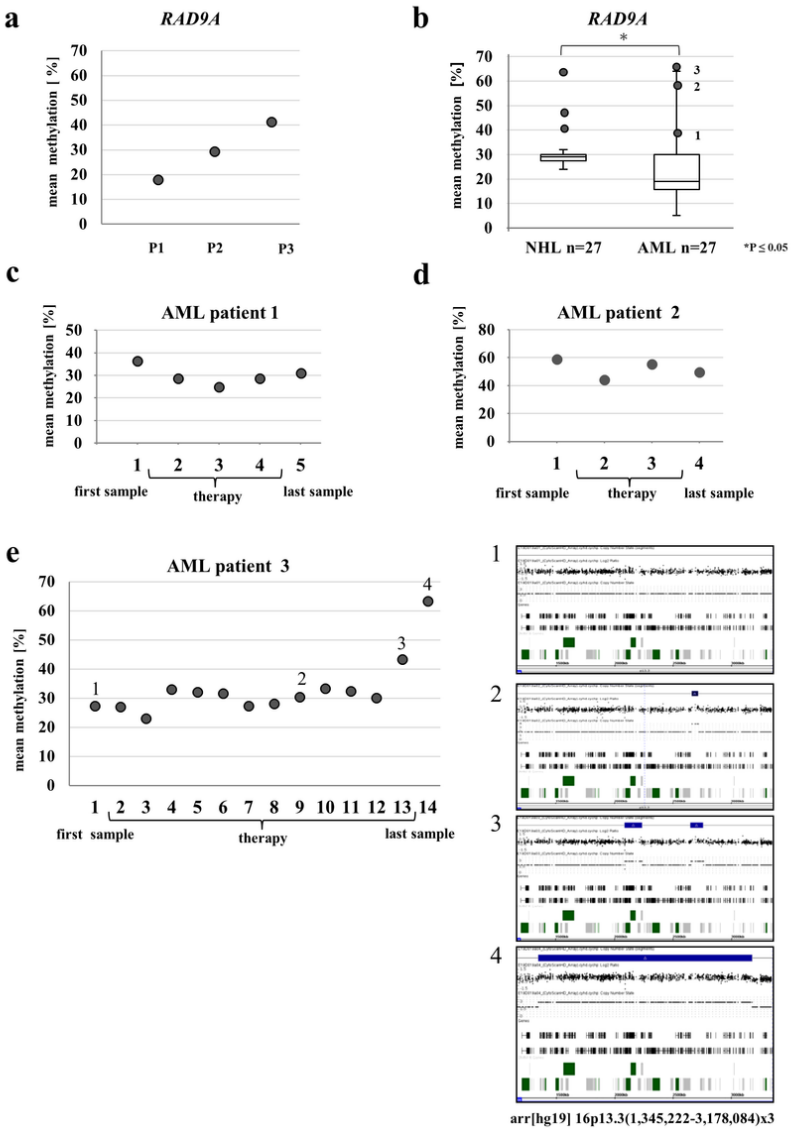

Figure 2

RAD9A methylation in the bone marrow of leukemia patients and selected AML patients during therapy. (a) Patient 1 (P1) with pre-ALL and a Philadelphia chromosome in <10% of analyzed bone marrow cells displayed mean methylation of 18%. Patient 2 (P2) with AML and 50% bone marrow cells with abnormal karyotype displayed 29% RAD9A methylation. Patient 3 (P3) with plasmablastic lymphoma and 60% cells showing complex aberrations consisting of a hypodiploid clone (28%) and a hyperdiploid line (32%) show 41% RAD9A methylation. (b) Analysis of 27 NHL and 26 AML bone marrow samples revealed overall mean methylation of 30% for the RAD9A intron 2 site. In a few patients, the mean methylation was elevated. (c-e) Methylation profile of RAD9A in 3 AML patients during therapy. (e) Using a genome-wide SNP array four bone marrow samples of the AML patient 3 (1-4) were analyzed. Corresponding images from chromosome 16p13.3 display a progressive duplication of the 16p13.3(1,345,222-3,178,084) fragment in the last 3 samples (blue bars). The final duplicated region contains 106 genes of which 9 genes are involved in cancer (UBE2I, NUBP2, IGFALS, NTHL1, TSC2, PKD1, PDPK1, TCEB2, and TNFRSF12A).

Fig. 3

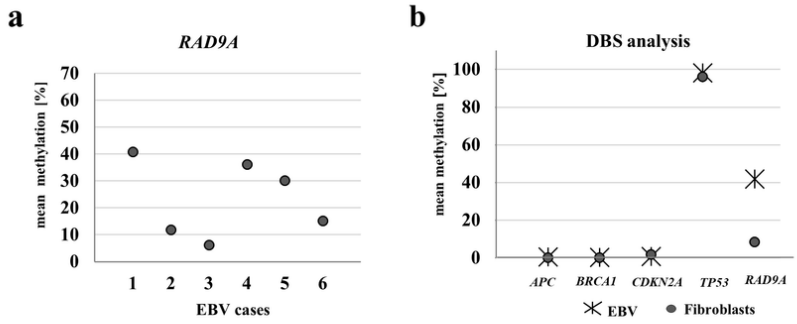

Figure 3

Mean RAD9A methylation in EBV-transformed lymphoblasts. (a) The mean methylation varied in six different EBV-transformed cell lines from 6% to 41%. (b) The DBS analysis of the EBV cell line with the highest methylation value exhibited 41% RAD9A methylation. In contrast, the methylation patterns of APC, BRCA1, CDKN2A, and TP53 in this cell line remained virtually unchanged after transformation. The mean methylation of RAD9A of the corresponding fibroblast cell line was 8%.

Fig. 4

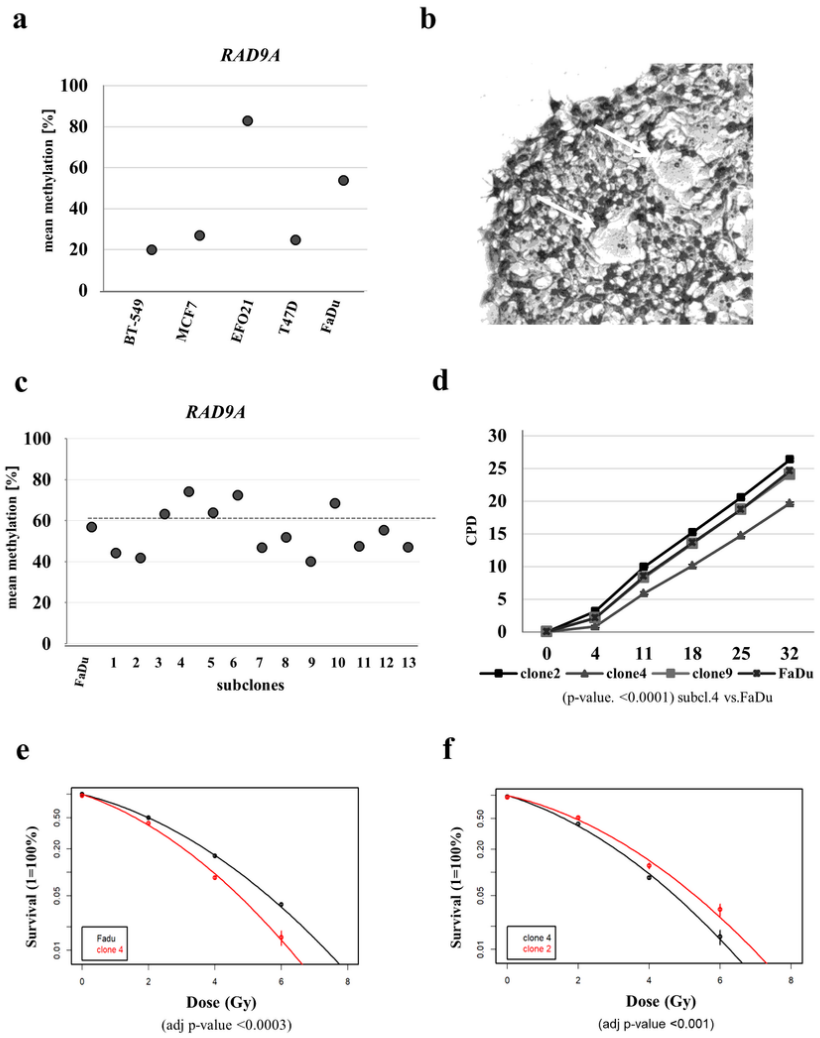

Figure 4

Methylation values for intron 2 of RAD9A in tumor cell lines and FaDu subclones. (a) Mean methylation values in BT-549, MCF7, EFO21, T47D and FaDu cell lines. (b) Crystal violet staining of an exemplary FaDu colony. Divergent cells are depicted by arrows. (c) Mean methylation of FaDu subclones. The highest values were determined in subclone 4 (75%) and subclone 6 (73%), the lowest values for subclone 9 (40%) and subclone 2 (42%). (d) Cumulative population doublings for subclones 2, 4, 9 and the parental FaDu cell line. Subclone 4 is delayed in growth (p-value. <0.0001). (b) Survival post radiation for the subclone 4, FaDu and (c) subclones 2 and 4. Clonogenic survival was calculated as the percentage of the non-irradiated controls and is shown as means +- S.D of three independent experiments. Linear quadratic fitting was performed, and results were compared using F-testing. Subclone 4 was significantly sensitive to radiation treatment in comparison to subclone 2 and parental FaDu cell line (adj p-value <0.001 and adj p-value <0.0003).

Fig. 5

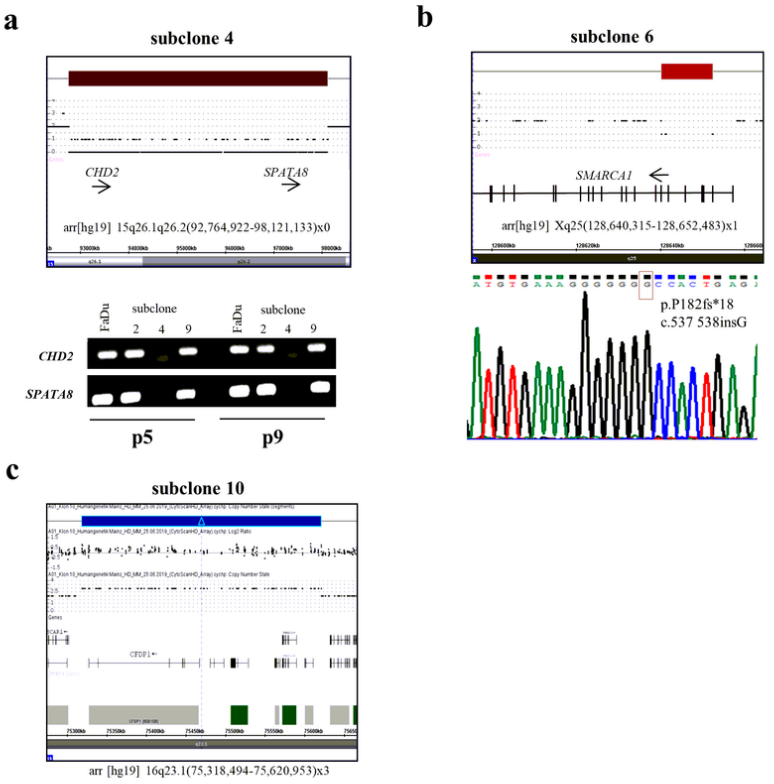

Figure 5

Mutation analysis of FaDu subclones 4, 6 and 10. (a) CHD2 and SPATA8 are homozygous deleted in subclone 4 (b). Homozygous mutation (deletion and stop mutation) is shown for SMARCA1 in subclone 6. Analysis was conducted in two different passages (p5 and p9)(c) The subclone 10 displayed a 302 kb duplication (indicated as a blue bar) in 16q23.1(75,318,494-75,620,953).

Fig. 6

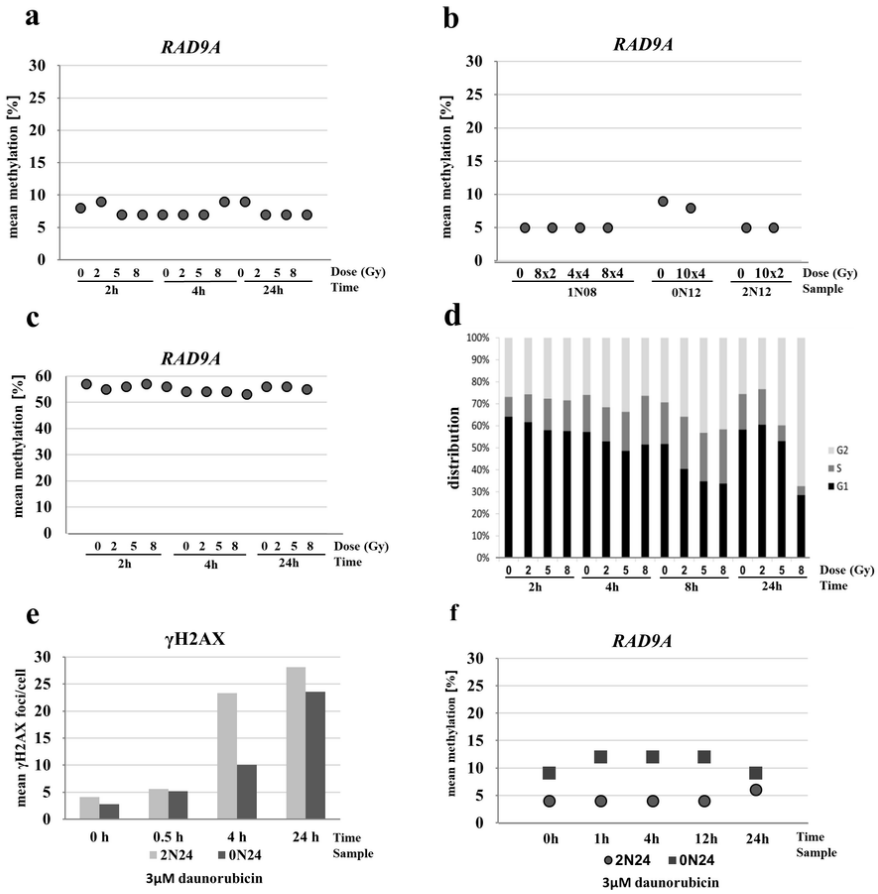

Figure 6

Effects radiation, and chemotherapeutics on RAD9A methylation. (a) Cell line 0N18 was analyzed at 15 min, 2, and 24 h after irradiation with 0 Gy, 2 Gy, 5 Gy, and 8 Gy, at each time point. Mean RAD9A methylation values remained virtually unchanged between 7% and 9%. (b) Fibroblast cell lines (0N12, 1N08, and 2N12) were irradiated in fractions of 8x 2 Gy, 4x 4 Gy, 10x 2 Gy, 8x 4 Gy, and/or 10x 4 Gy within 20 days. Mean RAD9A methylation remained constant at 5% in 1N08 and 2N12, and at 8-9% in 0N12. (c) Exponentially growing FaDu tumor cells were analyzed at 2, 4, and 24 h after irradiation with a single dose of 0 Gy, 2 Gy, 5 Gy, and 8 Gy. Mean RAD9A methylation varied within a narrow range between 54% and 57%. There was no difference between irradiated and non-irradiated cells. (d) Cell cycle analysis of FaDu cell line after treatment. The cell line was treated with increasing doses from 2 to 8 Gy. DNA was extracted at 2, 4, 8, and 24 h post-radiation. Shifts in the cell cycle phase indicate an arrest in the G2/M checkpoint. (e) Treatment of primary fibroblasts in a subconfluent state with 3μM daunorubicin. Incorporation and toxicity of daunorubicin in corresponding samples show a time-dependent increase of γH2AX foci reflecting the DNA damage. (f) Examination of mean methylation of RAD9A at 0, 1, 4, 12 and 24 h post-treatment showed no changes in methylation in two independent fibroblast cell lines (2N24 and 0N24).

Supplementary Files

This is a list of supplementary files associated with this preprint. Click to download.

- SupplementaryTables.docx

- MarkerFaDuclone249spacenegativCDH2STAT8.tif
- SupplementaryreferencesS3Galetzkaetal.17.07.2020.docx